Monthly Notices
of the
ROYAL ASTRONOMICAL SOCIETY

Mon. Not. R. Astron. Soc. **424,** 1327–1334 (2012) doi:10.1111/j.1365-2966.2012.21316.x

The 'harder when brighter' X-ray behaviour of the low-luminosity active galactic nucleus NGC 7213

D. Emmanoulopoulos,[1⋆] I. E. Papadakis,[2,3] I. M. McHardy,[1] P. Arévalo,[4] D. E. Calvelo[1] and P. Uttley[5]

[1]*Physics and Astronomy, University of Southampton, Southampton SO17 1BJ*
[2]*Physics Department, University of Crete, PO Box 2208, 71003 Heraklion, Greece*
[3]*IESL, Foundation for Research and Technology, 71110 Heraklion, Greece*
[4]*Departamento de Ciencias Fisicas, Universidad Andres Bello, Av. Republica 252, Santiago, Chile*
[5]*Sterrenkundig Instituut Anton Pannekoek, University of Amsterdam, Postbus 94249, 1090 GE, Amsterdam, the Netherlands*

Accepted 2012 May 15. Received 2012 May 14; in original form 2012 April 16

ABSTRACT

We present the first robust evidence of an anticorrelation between the X-ray photon index, Γ, and the X-ray luminosity in a single low-luminosity active galactic nucleus (LLAGN), NGC 7213. Until today, such anticorrelation trends have been seen only in large samples of LLAGN that span a wide range of X-ray fluxes, although the opposite behaviour (i.e. a positive correlation between Γ and X-ray luminosity) has been extensively studied for individual X-ray bright active galactic nuclei. For NGC 7213, we use the long-term X-ray monitoring data of the *Rossi X-ray Timing Explorer* (*RXTE*), regularly obtained on average every two days from 2006 March to 2009 December. Based on our X-ray data, we derive the Γ versus flux and the hardness ratio versus flux relations, indicating clearly that NGC 7213 follows a 'harder when brighter' spectral behaviour. Additionally, by analysing radio and optical data, and combining data from the literature, we form the most complete spectral energy distribution (SED) of the source across the electromagnetic spectrum yielding a bolometric luminosity of 1.7×10^{43} erg s^{-1}. Phenomenologically, the SED of NGC 7213 is similar to that of a low-ionization nuclear emission-line region. The robust anticorrelation trend that we find between Γ and X-ray luminosity together with the low accretion rate of the source, 0.14 per cent that of the Eddington limit, makes NGC 7213 the first LLAGN exhibiting a similar spectral behaviour with that of black hole X-ray binaries in the 'hard state'.

Key words: accretion, accretion discs – galaxies: individual: NGC 7213 – galaxies: nuclei – galaxies: Seyfert – X-rays: binaries – X-rays: galaxies.

1 INTRODUCTION

NGC 7213 ($z = 0.005\,839$) is a face-on Sa galaxy hosting an active galactic nucleus (AGN). It has been classified as a type I Seyfert by Phillips (1979), based on its Hα line width (full width at zero intensity of 13 000 km s^{-1}), but also as a low-ionization nuclear emission-line region (LINER) by Filippenko & Halpern (1984), based on the study of a variety of optical emission lines which were observed to have a full width at half-maximum of 200–2000 km s^{-1}.

NGC 7213 hosts a black hole with a mass of about 10^8 M$_\odot$ (Woo & Urry 2002). Its bolometric luminosity of $L_{\rm bol} = 9 \times 10^{42}$ erg s^{-1} (Starling et al. 2005) suggests a rather low accretion rate of 0.07 per cent of the Eddington luminosity ($L_{\rm Edd}$). As noted by Lobban et al. (2010), this value is intermediate between those usually found in type I Seyfert galaxies and LINERs and it is significantly less than the predicted 2 per cent $L_{\rm Edd}$ 'critical' rate at which the 'soft state' transition appears in black hole X-ray binaries (BHXRBs; Maccarone 2003). Finally, based on its radio properties, NGC 7213 belongs to a rare class of extragalactic sources lying between the radio-loud and radio-quiet AGN (it is one of the 20 sources of the Roy & Norris 1997 sample). In this sense, it can be considered as an extragalactic analogue of the Galactic 'hard state' sources.

The X-ray spectral behaviour NGC 7213 is also peculiar. Starling et al. (2005) using the Reflection Grating Spectrometer on board *XMM–Newton* found several emission features with no absorption lines, in contrast to what is usually observed in type I Seyfert galaxies. The absence of a Compton reflection component from either neutral or ionized material together with the lack of a relativistic Fe Kα line suggests that the inner, optically thick accretion disc in the source may be absent (Lobban et al. 2010), and replaced by an

⋆E-mail: D.Emmanoulopoulos@soton.ac.uk

advection-dominated accretion flow (ADAF; Starling et al. 2005). This possibility further supports the 'hard state' interpretation of the source.

Recently, Bell et al. (2011) used radio and X-ray observations of NGC 7213, from a long-term observing campaign consisting of several years, to search for correlated X-ray and radio variations that might originate in the so-called 'Fundamental Plane of black hole accretion' (Merloni, Heinz & di Matteo 2003; Körding, Falcke & Corbel 2006). Bell et al. (2011) showed that the average radio and X-ray luminosities fitted well with the global Fundamental Plane, consistent with a 'hard state' identification of this AGN. However, the X-ray versus radio correlation within the monitoring period was weak, with significant intrinsic scatter away from the Plane.

Numerous studies in the past have shown that the X-ray photon index, Γ, correlates with the accretion rate, defined as $\xi = L_{\rm X}/L_{\rm Edd}$ (where $L_{\rm X}$ is usually the 2–10 keV X-ray luminosity) in both AGN and BHXRBs. For example, Shemmer et al. (2006) showed that Γ and ξ are positively correlated, using data for a sample of 30 quasars, while Sobolewska & Papadakis (2009) found that the same positive correlation holds when one studies the spectral variations of individual, luminous Seyfert galaxies. However, the positive $\Gamma-\xi$ correlation may not hold in less luminous AGN. In fact, Gu & Cao (2009) found an anticorrelation between Γ and ξ in a sample of 55 low-luminosity AGN (LLAGN), and Younes et al. (2011) reached a similar conclusion for a sample of 13 optically selected LINERs.

Wu & Gu (2008) performed a detailed spectral study for six BHXRBs and found that Γ anticorrelates with ξ below a 'critical' value of $\log(\xi_{\rm crit}) = -2.1 \pm 0.2$. At higher accretion rates, Γ and ξ are positively correlated. Similar conclusions were also reached recently by Sobolewska et al. (2011). The Γ–ξ relation in AGN may also change from negative to positive at a similar 'critical' value, as suggested by Wu & Gu (2008) and Constantin et al. (2009). This analogous behaviour between AGN and BHXRBs reinforces the interpretation that LLAGN are analogues of the 'hard state' BHXRBs while luminous Seyferts and quasars are the equivalents of the 'soft state' BHXRBs. On a first look, during the 'hard state', BHXRBs appear to have a constant hardness ratio, in the commonly used hardness–intensity diagrams (e.g. Belloni et al. 2005). Nevertheless, a detailed analysis of the lowest luminosity regime of this state, known also as the 'low-hard' state, clearly exhibits an increase of the hardness ratio for increased fluxes, corresponding to an anticorrelation between Γ and ξ (Heil, Vaughan & Uttley 2012).

The negative and the positive correlations between Γ and ξ, occurring below and above $\xi_{\rm crit}$, respectively, may be indicative for some 'switch' in the emission mechanism as the source's accretion rate increases above $\xi_{\rm crit}$. In fact, it has been suggested (Wu & Gu 2008; Constantin et al. 2009; Younes et al. 2011) that this transition could indicate the passage from an ADAF (Narayan & Yi 1994; Esin, McClintock & Narayan 1997) to a standard disc (but see Sobolewska et al. (2011) for alternative explanations as well).

The positive correlation relation between Γ versus ξ in AGN has been firmly established statistically by considering either samples of numerous sources (e.g. Shemmer et al. 2006) or large data sets for a few individual sources (e.g. McHardy, Papadakis & Uttley 1999; Lamer et al. 2003; Sobolewska & Papadakis 2009). However, thus far the Γ–ξ anticorrelation has been established using only short X-ray observations of numerous different sources (Constantin et al. 2009; Gu & Cao 2009; Younes et al. 2011), while it has never been observed in a single source.

In this work, we use long-term, monitoring *RXTE* data, and present, for the first time, conclusive evidence for such an anti-correlation for an individual LLAGN, namely NGC 7213. We also use archival and proprietary data to construct its average spectral energy distribution (SED), and compare it with the average SED of luminous AGN and LINERs. In Section 2 we refer to the observations and data reduction procedures and in Section 3.1 we present our results consisting of the Γ versus flux relation and the SED of the source. Finally, a discussion together with a summary can be found in Section 4. The cosmological parameters used throughout this paper are: $H_0 = 70\,{\rm km\,s^{-1}\,Mpc^{-1}}$, $\Omega_\Lambda = 0.73$ and $\Omega_{\rm m} = 0.27$, yielding a luminosity distance to NGC 7213 of 22.12 Mpc (for a corrected redshift $z_{\rm corr.3K} = 0.005\,145$ to the reference frame defined by the 3-K cosmic microwave background radiation). This value of the luminosity distance appears to be fully consistent with the redshift-independent Tully–Fisher distance (Tully 1988).

2 OBSERVATIONS AND DATA REDUCTION

2.1 X-ray data

NGC 7213 has been observed regularly by the *Rossi X-ray Timing Explorer* (*RXTE*) (proposal numbers: 92119, 93139, 94139 and 94342) from 2006 March 3, 02:57:41 (UTC) to 2009 December 30, 00:18:37 (UTC) (on-time: 800506 s). This is the complete set of X-ray observations of NGC 7213, obtained by *RXTE*, extending the X-ray data of Bell et al. (2011) by an additional 100 d. In order to form the most homogeneous long-term data set, we use data obtained only by the proportional counter array 2 (PCU 2), one of the five xenon proportional counters forming the proportional counter array (Jahoda et al. 1996). PCU 0 and 1 have lost their propane layer, resulting in an increased background rate as well as a different detector gain, and PCU 3 and 4 are usually switched off due to discharge problems.

The Standard-2 (Std2: data with an accumulation rate of 16 s) PCU 2 data (822 files in total) are extracted and processed using `ftools` (Blackburn 1995) included in HEASOFT (ver. 6.11.1), following the standard reduction procedures, provided by the *RXTE* Guest Observer Facility (GOF). For each observation we create a filter file, assembling the scientifically important parameters, using the script XTEFILT and then by using the `ftool` FMERGE we merge them all in a single 'master' filter file. Then, based on this file, we extract the useful observing time periods, known as good time intervals (GTIs), using the `ftool` MAKETIME having the following observational constraints: elevation angle greater than 10°, a pointing offset of less than $0\overset{\circ}{.}02$, electron contamination less than 0.1, time since south Atlantic anomaly between 0 and 30 min and time since PCU breakdowns less than -150 s or greater than 600 s. Finally, for each Std2 observation, a synthetic background model file is created with the `ftool` PCABACKEST using the 'faint background model'.

For the production of the background-subtracted light curves, in the 2–4, 5–10 and 2–10 keV energy bands, we use the `ftool` SAEXTRCT to produce the 'source-plus-background' and 'background' light curves for each energy band, respectively. We select events obtained during the GTIs registered only from the top xenon layer (X1L and X1R) of PCU 2, optimizing in this way the signal-to-noise ratio. Then the corrected background-subtracted light curves are produced by using the `ftool` LCMATH in units of count rate. In order to produce a total long-term X-ray light curve in the 2–10 keV energy range, in units of flux, i.e. erg s^{-1} cm^{-2}, we extract for each Std2 observation, and the corresponding synthetic background file, a spectrum together with the PCU 2's response using

Table 1. The radio, near-IR and optical mean flux values of NGC 7213.

Energy band	Flux (mJy)
1.344 GHz	121.3 ± 2.2
1.384 GHz	112.4 ± 9.3
2.386 GHz	114.9 ± 3.6
2.496 GHz	98.1 ± 4.1
4.8 GHz	135.8 ± 8.3
8.64 GHz	150.6 ± 24.3
17 GHz	140.4 ± 3.9
19 GHz	128.5 ± 4.1
12.27 μm*	235.8 ± 128.4
11.25 μm*	232.9 ± 144.5
10.49 μm*	239.1 ± 22
5500 Å	0.49 ± 0.18
4400 Å	0.73 ± 0.15

*The near-IR measurements taken from Hönig et al. (2010) and Asmus et al. (2011) as explained in the text.

again the `ftool` SAEXTRCT and the script PCARSP, respectively. Again, we select events obtained during the GTIs which are registered only from the top xenon layer of PCU 2. The resulting spectra are then grouped so that each spectral bin contains at least 30 counts, using the `ftool` task GRPPHA.

Using the X-ray-fitting package XSPEC (ver. 12.7.0; Arnaud 1996) we fit to each X-ray spectrum a power-law model assuming photoelectric absorption (XSPEC model `wabs`), of a fixed interstellar column density of $N_{\rm H} = 1.1 \times 10^{20}\,{\rm cm}^{-2}$ (estimated using the `ftool` NH, after Kalberla et al. 2005). Finally, after fixing the fitting parameters (i.e. photon index and normalization) to their best-fitting values, we obtain the flux values in the 2–10 keV energy range using the convolution model `cflux`. The errors in the spectral indices and fluxes indicate their 68.3 per cent confidence range, corresponding to a $\Delta\chi^2$ of 1, unless otherwise stated.

2.2 Spectral energy distribution data

In order to construct the SED of NGC 7213, we analyse long-term monitoring radio and optical data. Below we describe the data analysis procedures for these observations. We also use the published near-infrared (IR), nuclear fluxes of Hönig et al. (2010) and Asmus et al. (2011) at 12.27 and 11.25 and 10.49 μm (these fluxes are listed in Table 1 with an asterisk). Finally, we also considered the results from a 130-ks *XMM–Newton* observation obtained during 55146–55148 MJD (obs ID: 0605800301; Emmanoulopoulos et al., in preparation), the 4.5 years' average *Swift* -BAT spectrum (as reported in entry 1185 of table 2 in Cusumano et al. 2010), and the recent 0.1–100 GeV *Fermi*-LAT upper limit (Lobban et al. 2010).

2.2.1 Radio data

We searched the Australian Telescope Online Archive (ATOA) for Australian Telescope Compact Array (ATCA) observations of the location of NGC 7213, selecting a range that covered as many frequencies as possible, opting for the longest duration observation(s) in each case (sometimes yielding multiple useful files, as in the case of 5–10 GHz). While attempts were made to process all designated files, the highest available frequencies, greater than 20 GHz, did not yield useful images. The final data set used in this work was comprised of 21 ATCA observations, from four projects C782, C1803, C1532 and C1392.

The primary calibrator for all these data sets was PKS 1939−6342 (PKS B1934−638). C782 includes observations from 1999 March 3 and frequencies of 1344 MHz [0.3 h on-source, an average beam size (ABS) of $64.7 \times 7.0\,{\rm arcsec}^2$), 1384 MHz (8.5 h on-source, ABS $= 21.6 \times 7.2\,{\rm arcsec}^2$) and 2496 MHz (8.8 h on-source, ABS $= 7.6 \times 4.9\,{\rm arcsec}^2$), with the antennas in configuration 6C (a minimum baseline length of 153 m and maximum of 6 km). The secondary calibrator used was PJS J2214−3835 (PKS B2211−388A). C1803 included observations from 2008 April 21 and 23 at 1384 and 2386 MHz, with 0.15 and 0.1 h on-source, respectively. The antenna configuration was 6A (a minimum baseline length of 337 m and maximum of 5939 m) and the secondary calibrator used was PKS J2235−4835 (PKS B2232−488). C1532 contributed all our 4800 MHz (ABS $= 17.3 \times 1.8\,{\rm arcsec}^2$) and 8640 MHz (ABS $= 9.64 \times 1\,{\rm arcsec}^2$) data, with observations covering the dates 2008 January 5, 24, April 12, November 4 and 20 with on-source durations of 1.48, 1.7, 1.5, 2.29 and 1.49 h, respectively. The secondary calibrator used in all cases was PKS J2218−5038 (PKS B2215−508) and antennas were always in configuration 6A. Finally, C1392 provided our highest frequency ATCA data, at 17 GHz (ABS $= 35.5 \times 27.55\,{\rm arcsec}^2$) and 19 GHz (ABS $= 29.15 \times 22.8\,{\rm arcsec}^2$). Two observations are used from 2009 September 29 and 30 with 0.02 and 0.03 h on-source, respectively. The secondary calibrator was PKS J2248−3235 (PKS B2245−328) and the antenna configuration was H75 (a minimum baseline of 31 m and maximum of 4408 m).

Once imaging was complete, point-source fitting is used to measure flux density at the position of NGC 7213 RA(1950) $= 22^{\rm h}09^{\rm m}16\overset{\rm s}{.}26$ and Dec.(1950) $= -47^\circ09'59\overset{''}{.}95$. All data and image processing is carried out in the radio interferometry data reduction package MIRIAD (Sault, Teuben & Wright 1995).

2.2.2 Optical data

We used the ANDICAM instrument mounted on the 1.3-m telescope SMARTS (Smart and Moderate Aperture Research Telescope System) in Chile to observe NGC 7213 in the optical *B* (4400 Å) and *V* (5500 Å) bands. Observations were performed between 2006 August and 2011 August, every 4 d and during each observations two 60-s exposure frames in the *B* band and two 30-s exposures in the *V* band were obtained when the target was visible. After discarding the 'bad seeing' nights, 266 epochs are accumulated in each band. The field of view of ANDICAM is $6 \times 6\,{\rm arcmin}^2$, covering both the entire host galaxy and a few bright stars, and the pixel size is 0.37 arcsec pixel^{-1}. The typical seeing during the campaign was about 1.5 arcsec. The data reduction for both the *B* and *V* band images is the same.

Since NGC 7213 host galaxy is a face-on spiral with a bright nucleus compared to the AGN, galaxy subtraction has to be performed to determine the pure AGN flux. To model correctly the large-scale structure we use the data analysis algorithm galfit (ver. 3.0; Peng et al. 2010), fitting a Nuker function. After the fitting, a bright ring 10 arcsec from the nucleus is left together with some spiral structure inwards of the ring and a resolved core. The core is subtracted using a Moffat function, leaving a residual nuclear peak consistent with the stellar point-spread function (PSF), which we identified with the AGN. Aperture photometry is performed with the task DAOPHOT of the IRAF (ver. 2.15) software system (Tody 1993) on the stars of the original image and the modelled nuclear PSF to determine its

relative brightness. In order to estimate the flux, the reference stars in turn are calibrated taking their average aperture magnitudes over all reported photometric nights when observations were carried out, corrected for airmass extinction. The average nuclear fluxes that are obtained in this way are 5×10^{-12} erg s^{-1} cm^{-2} at 4400 Å and 3×10^{-12} erg s^{-1} cm^{-2} at 5500 Å, while the fractional root-mean-square variability amplitude (including observational noise and intrinsic variability) is around 1 erg s^{-1} cm^{-2} for both bands, respectively.

3 RESULTS FOR NGC 7213

3.1 The X-ray flux–photon index relation in NGC 7213

The upper panel of Fig. 1 shows the 2–10 keV, X-ray light curve of NGC 7213. One can observe variations on time-scales of days and weeks, superimposed on a flux-decreasing trend, from the start to the end of the monitoring campaign. Each measurement on this plot corresponds to one *RXTE* pointing, having a mean duration of 1.06 ± 0.25 ks (the error estimate corresponds to the standard deviation of the exposure times of individual observations). On average, *RXTE* observed the source every ∼2.3 d, except from the period between 54982 and 55077 MJD (indicated by the double-headed arrow in the upper panel of Fig. 1), where observations were performed around every half a day. Observations with large uncertainties, e.g. around (53797+450) MJD, correspond to exposure times of less than 0.9 ks.

The lower panel of Fig. 1 shows the evolution of Γ as a function of time. In order to investigate any possible relationship between the flux and Γ, we group both data sets in bins of 45 consecutive observations (each bin is then ∼100 d long). For the intense monitoring period (1185–1280 MJD −53797) we apply the same sampling scheme by selecting only the observations that are separated around 2.3 d and then bin them in bins of 45 consecutive observations. In this way we ensure that the resulting X-ray flux and the photon index range are represented by an equal number of observations, avoiding the possibility that the larger number of observations in the intense monitoring period could drive the resulting flux/photon index relation. We estimate a weighted mean and a weighted error (e.g. Bevington & Robinson 1992) for both the flux and Γ in each bin. Fig. 2 shows the resulting average X-ray flux and Γ values, plotted against each other, unveiling a clear 'harder when brighter' behaviour.

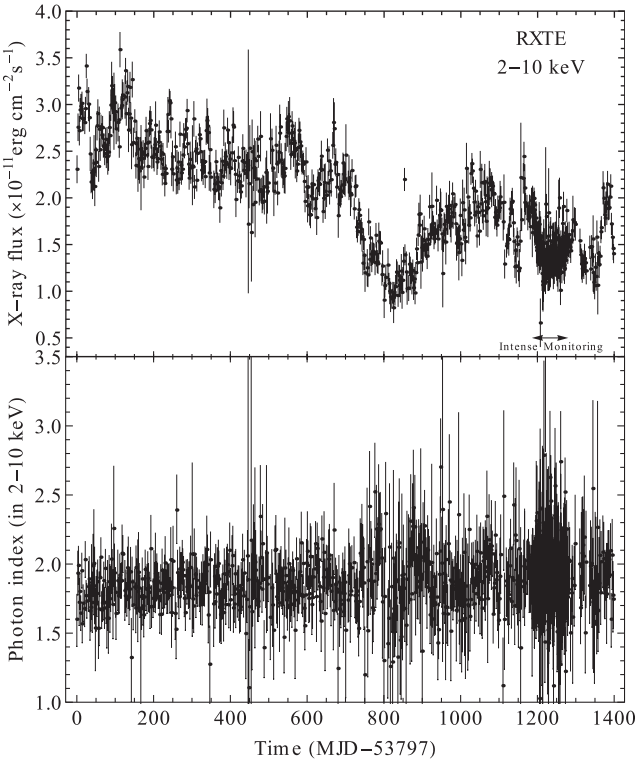

Figure 1. The *RXTE* results of NGC 7213. Top panel: the long-term light curve in the 2–10 keV energy range. The double-headed arrow indicates the intense monitoring period between 54982 and 55077 MJD. Lower panel: the photon index of each pointing observation as a function of time.

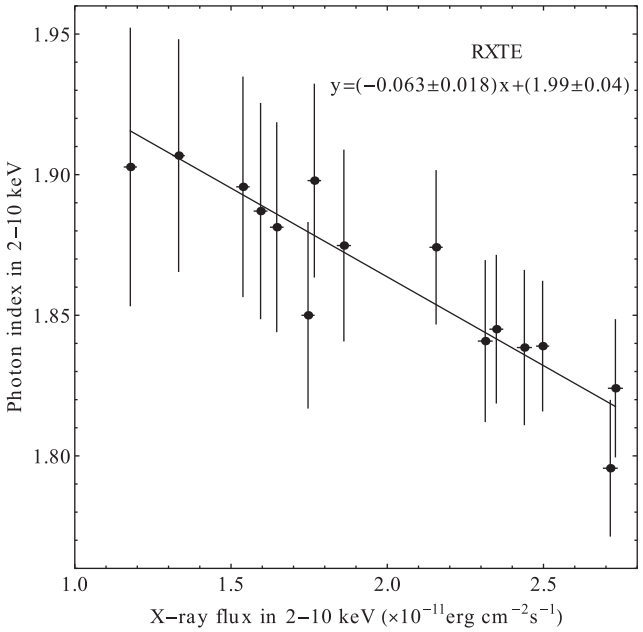

Figure 2. The average photon index versus the average X-ray flux of NGC 7213 in bins of 45 consecutive observations. The data suggest a 'harder when brighter' relation. The solid line indicates the best-fitting linear model to the data taking into account the uncertainties in both coordinates.

In order to quantify this anticorrelation, we first compute the Kendall's τ rank correlation coefficient (Press et al. 1992), using the data plotted in Fig. 2, yielding $\tau = -0.81$ with a null-hypothesis probability of 2.6×10^{-5}. This result shows that the anticorrelation between the spectral slope and the flux is highly significant. Then, we fit to the data a linear model, $(y = \alpha x + \beta)$, considering the uncertainties in both coordinates (Press et al. 1992). The best-fitting model yields a slope of $\alpha = -0.063 \pm 0.018$ and an intercept of $\beta = 1.99 \pm 0.04$ with a χ^2 merit function of 2.90 for 13 degrees of freedom (dof) having a null-hypothesis probability of 1.7×10^{-3}. Fig. 3 shows the confidence contour (the solid black line) used to estimate the one-standard deviation uncertainties on the best-fitting parameters corresponding to an ellipsoidal region with a χ^2 of 3.90 ($\Delta\chi^2 = 1$ from the minimum for 1 dof). In the same plot, we also show the contours for confidences of 95 and 99 per cent as well as the 68.3 per cent joint confidence contour for both the slope and the intercept with the latter corresponding to a $\Delta\chi^2 = 2.30$ from the minimum for 2 dof. A simple linear regression model, taking into account only the photon index uncertainties, yields equivalent results: $\alpha = -0.063 \pm 0.008$ and $\beta = 1.99 \pm 0.02$ ($\chi^2 = 2.90$ for

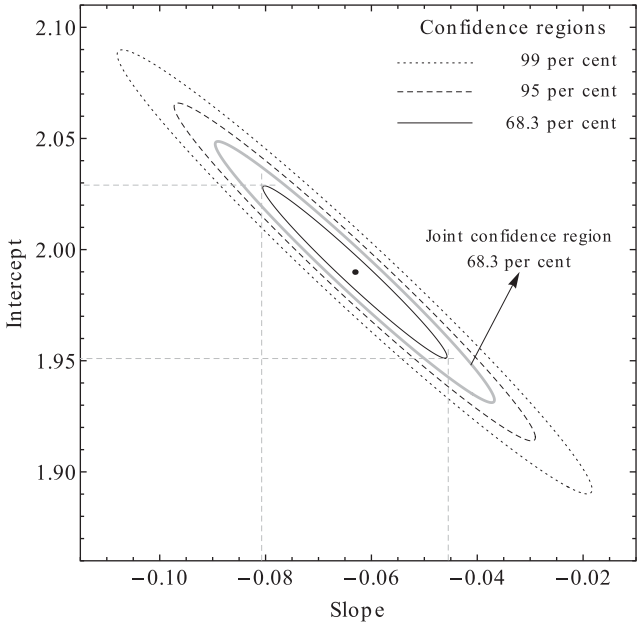

Figure 3. The confidence contours for the best-fitting model of Fig. 2 taking into account the uncertainties in both coordinates. The black thin lines correspond to the 99, 95 and 68.3 per cent confidence contours and represent the ellipsoids having from the minimum a $\Delta\chi^2$ of 6.63, 3.84 and 1, respectively, for 1 dof. The grey thick line corresponds to the 68.3 per cent joint confidence contour for the slope and the intercept having from the minimum a $\Delta\chi^2$ of 2.30, for 2 dof. The horizontal and vertical dashed grey lines correspond to the tangents of the 68 per cent confidence region yielding the 68 per cent uncertainty ranges of the slope and the intercept, respectively.

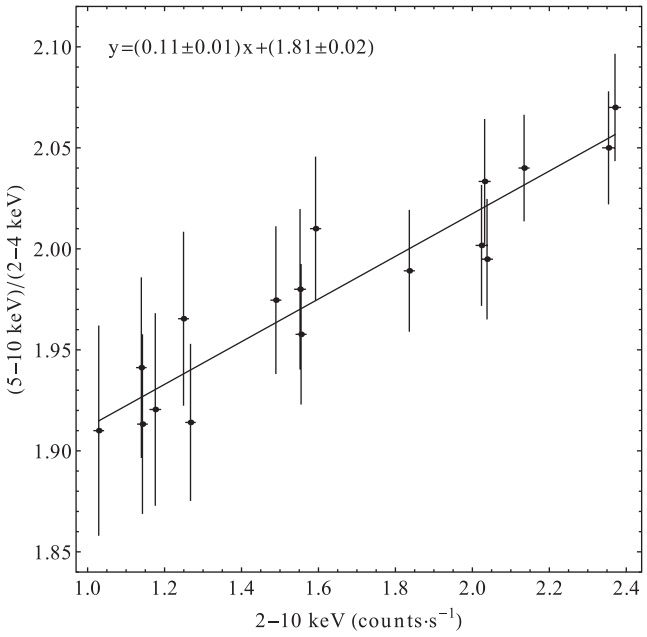

Figure 4. Hardness-ratio plot of the count rate in (5–10 keV)/(2–4 keV) versus 2–10 keV. The bin size corresponds to 50 consecutive observations. The solid line indicates the best-fitting linear model to the data taking into account the uncertainties in both coordinates. The positive slope implies a 'harder when brighter' X-ray spectral behaviour.

13 dof). The resulting χ^2, from both methods, are relatively small, indicating that the estimated errors on the average Γ within each bin may be slightly overestimated. We therefore repeat the fit and this time we fit to the data a linear model following the 'ordinary least-squares regression of Y on X' routine of Isobe et al. (1990) which does not take into account the error on the data. The best-fitting results from these routines are consistent, within the quoted errors, with the previous results yielding: $\alpha = -0.072 \pm 0.008$ and $\beta = 2.00 \pm 0.02$.

We have performed several sanity checks in order to test the sensitivity of our results to the binning scheme. We have considered alternative binning of 20, 60 and 100 consecutive observations as well as considering all the data from the intense monitoring period. Also, we have performed data resampling using jackknifing (Shao & Tu 1995) by selecting randomly subsamples from the data set and binning them in the flux/photon index plane. All the results are extremely consistent with each other. Finally, in order to ensure that the overall anticorrelation trend is not induced by any sort of statistical dependence between the flux and Γ (e.g. Vaughan & Edelson 2001), we measured the eccentricity and the orientation of the χ^2 contour plots of the fits, used to derived the uncertainties of the fluxes and slopes. The 68 per cent ellipsoids have an average eccentricity of 0.91 ± 0.03 and they are tilted on average by an angle of $79^\circ \pm 2^\circ$ counter-clockwise from the horizontal (flux) axis favouring, if at all, trends moving the opposite direction, i.e. a positive correlation between the flux and Γ. We therefore conclude that for NGC 7213, contrary to what is observed in other luminous Seyfert galaxies, the X-ray photon index anticorrelates with the X-ray flux.

3.2 Hardness-ratio analysis

A completely model-independent way to check for the validity of the above-mentioned anticorrelation behaviour is by estimating the hardness ratio from the X-ray light curves. After binning the light curves in bins of 50 consecutive observations, we estimate the hardness ratio (5–10 keV)/(2–4 keV) versus the overall count rate in 2–10 keV. In Fig. 4 we plot the corresponding estimates, showing a clear increasing trend which implies that the X-ray behaviour of the source becomes 'harder' when the source gets brighter.

We can now fit to the hardness-ratio data a linear model, ($y = \alpha x + \beta$), taking into account the errors in both coordinates (as in Section 3.1). The best-fitting model has a slope of $\alpha = 0.11 \pm 0.01$ and an intercept of $\beta = 1.81 \pm 0.02$, yielding a χ^2 of 4.31 for 15 dof having a null-hypothesis probability of 3.4×10^{-3}. Since the 99 per cent confidence interval for the slope is (0.07, 0.14), the null hypothesis can be rejected at the 1 per cent significance level. Finally, the value of t-statistic that we get from the data is 10.1,[1] corresponding to a probability of getting such a value from chance alone equal to 4.6×10^{-8}. Therefore, we can robustly conclude that the best-fitting slope is significantly different from zero.

3.3 The nuclear broad-band spectral energy distribution

The average SED of NGC 7213 (in νL_ν representation) is shown in Fig. 5 (both panels) with black symbols corresponding to flux estimates (listed in Table 1) derived in this work and grey symbols to archival data. The error bars correspond to the standard deviation around the mean flux, at a given frequency, whenever multiple observations from different epochs are available. In this way, the error bars are indicative of the actual variability of NGC 7213 (the

[1] The value of t-statistic is $t_{15,\,0.005} = 2.95$.

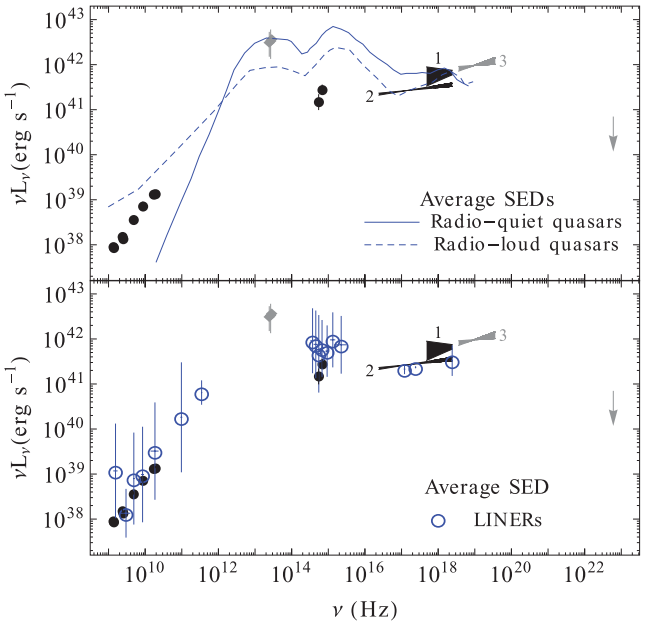

Figure 5. The SED of NGC 7213. For both panels, black symbols correspond to flux density estimates derived in this work and grey symbols correspond to archival data. The enumerated symbols 1, 2 and 3 correspond to the average *RXTE* spectrum (depicting the long-term variations), *XMM–Newton* and *Swift* -BAT spectrum, respectively. The grey arrow corresponds to the *Fermi* -LAT upper limit in the 0.1–100 GeV energy range. Top panel: the SED of NGC 7213 together with the average SEDs of radio-quiet and radio-loud quasars shown with the blue solid and dashed lines, respectively (taken from Elvis et al. 1994). Bottom panel: the SED of NGC 7213 together with the average SEDs of LINERs shown with blue open circles (taken from Eracleous et al. 2010).

actual uncertainty of single-pointing observations is much smaller than the symbol size). The average flux from the ensemble of *RXTE* observations in the 2–10 keV energy range is shown by symbol 1, and corresponds to a power law having normalization of $(6.51 \pm 3.73) \times 10^{-3}$ photons $s^{-1}\,cm^{-2}\,keV^{-1}$ (at 1 keV) and a photon index of 1.87 ± 0.23. The bow tie 2 indicates the 0.1–10 keV spectrum from the *XMM–Newton* observation (Emmanoulopoulos et al., in preparation), which is broadly consistent with a power law with a normalization of $2.99^{+0.06}_{-0.03} \times 10^{-3}$ photons $s^{-1}\,cm^{-2}\,keV^{-1}$ (at 1 keV) and a photon index of $1.88^{+0.04}_{-0.02}$. The bow tie 3 indicates the average flux estimate registered by the *Swift*-BAT instrument, between 15 and 150 keV, corresponding to a power law with normalization[2] $5.4^{+3.1}_{-2.0} \times 10^{-3}$ photons $s^{-1}\,cm^{-2}\,keV^{-1}$ (at 1 keV) and a photon index of $1.82^{+0.13}_{-0.12}$. Finally, the 0.1–100 GeV the *Fermi*-LAT upper limit, assuming a photon index of 1.75, is 3×10^{-9} photons $s^{-1}\,cm^{-2}$, as indicated by the arrow at 0.25 GeV (mean energy of the *Fermi*-LAT energy band).

The mean SED of NGC 7213 is shown in Fig. 5. This is true even for the *RXTE* and *Swift*- BAT data, since at these flux levels the contribution of any host galaxy emission should be minimal, especially in the *Swift*-BAT band, as well as for the optical data, where we have carefully discarded the host galaxy contribution from our measurements. Also, note that the optical *RXTE* and *Swift*-BAT data plotted on this figure are indicative of the source flux averaged over many years, which are largely overlapping. On the other hand, the beam size of the radio observations is rather large, due the short exposure times (Section 2.2). As a result, the observed radio fluxes we have used may be contaminated by radio emission from a substantial part of the host galaxy itself. However, our radio flux estimates, at least for the 4.8- and 8.6-GHz bands, are identical to the mean flux values reported by Bell et al. (2011), who used a beam size of 0.5 arcsec for a 12-h integration time. In addition, the observed variability at all radio bands indicates that most of the emission should originate from the nucleus itself. Detailed X-ray studies (e.g. Lobban et al. 2010; Emmanoulopoulos et al., in preparation), indicate that the intrinsic absorption towards the nuclear source in NGC 7213 is minimal in addition to the fact that the galaxy of NGC 7213 is face-on.

Consequently, the SED in Fig. 5 should be representative of the mean-intrinsic nuclear SED of NGC 7213. The blue solid and dashed line in the top panel of Fig. 5 indicates the average SED of radio-quiet and radio-loud quasars (Elvis et al. 1994), respectively, and the blue open circles in the bottom panel of the figure indicate the average SED of LINERs (Eracleous, Hwang & Flohic 2010). Their relative position is set by minimizing the distance of their logarithmic ordinates from those of NGC 7213's, at the same frequencies, weighted by their squared errors. Since the distance minimization procedure is done in the logarithmic plane, in this way we estimate effectively an optimum normalization for each average-SED. Our results suggest that it is the LINERs mean SED which fits best, within the NGC 7213's SED. We therefore conclude that the nuclear continuum emission of the source is indeed representative of the mean SED of nearby LINERs.

Despite the fact that the (archival) near-IR flux measurements of NGC 7213 (as shown in the bottom panel of Fig. 5) are representative of emission from a central region which is less than 0.35 arcsec in size, it is not clear whether they correspond to emission from the nuclear source itself. For example, if we indeed observe the active nucleus directly, without any significant absorption, the detected near-IR emission cannot be due to optical/ultraviolet (UV) nuclear emission being absorbed by the putative dusty, obscuring torus in this galaxy and re-emitted in the near-IR, because the average optical luminosity is significantly lower than the observed near-IR luminosity. On the other hand, NGC 7213 shows evidence of a starburst-driven wind (Bianchi et al. 2008) and hosts a star-forming ring few kpc away from the nucleus. A clumpy torus with toroidal shape (Nenkova et al. 2008), having a small angular width parameter, can then explain the observed IR luminosity as being due to reprocessed radiation from star-forming regions, while the optical nuclear emission could escape unabsorbed through a torus hole. Note that LINERs are thought to have relatively hot yet normal main-sequence O stars (Shields 1992) able to heat the dust around them, something that strengthens even more the LINER interpretation of NGC 7213 SED.

The SED plotted in Fig. 5 is based on more observations of the nuclear source flux, and is spread over a larger frequency range, than the SED presented by Starling et al. (2005). We can therefore use it to derive a more accurate estimate of the nuclear bolometric luminosity. After interpolating the SED linearly in logarithmic space, we integrate it between 1.344 GHz and 3.63×10^{19} Hz (i.e. 150 keV) and derive $L_{\rm bol} = 1.7 \times 10^{43}$ ergs s^{-1}, yielding an accretion rate of 0.14 per cent of the Eddington limit.

4 DISCUSSION

We have analysed the long-term *RXTE* observations of NGC 7213 and found that this low-luminosity source exhibits a clear 'harder

[2] The flux value is consistent with the one derived from the maps of the fourth IBIS/ISGRI soft γ-ray survey catalogue (Bird et al. 2010).

when brighter' X-ray behaviour (Fig. 2). This is the first time when such a spectral variability behaviour is reported for either a 'low-' or 'high-'luminosity AGN, in contrast to what is observed in luminous Seyferts and quasars. We also constructed the average, nuclear SED of this source, using archival and proprietary data that we reduced, together with other measurements from the literature and we found that its shape closely resembles the mean SED of nearby LINERs. Finally, we provided a new measurement for the nuclear bolometric luminosity of NGC 7213, $L_{\rm bol} = 1.7 \times 10^{43}$ ergs s^{-1}, yielding a rather low accretion rate of 0.0014 (i.e. 0.14 per cent) of the Eddington limit.

The average, broad-band nuclear SED of NGC 7213 resembles that of LINERs (Fig. 5, bottom panel). In the average SEDs of radio-loud and radio-quiet AGN, the optical flux is quite higher than the X-ray flux. This is definitely not the case for this source, since the optical flux lies well below that of the X-rays. This is a very robust result, as both the optical and the X-ray data are based on long, monitoring observations, i.e. they show the average behaviour of the source over many years. Furthermore, Wu, Boggess & Gull (1983) noted that the UV excess for NGC 7213 should be extremely weak or absent, while both the recent *XMM–Newton* observations (Emmanoulopoulos et al., in preparation) and the *Suzaku* observations (Lobban et al. 2010) show no indication of the soft X-ray excess, which is typical in most luminous AGN. All these results strongly suggest that the 'big-blue bump' is missing in this source. This can be expected in a scenario in which the inner part of the geometrically thin and optically thick disc is missing in NGC 7213.

Our results suggest that the accretion rate of the source is significantly smaller (by a factor of 10) than the 'critical' rate at which accreting BHXRBs move from the 'hard' to the 'soft state'. Therefore, NGC 7213 could be the 'hard state' analogue of BHXRBs and, in fact, its 'harder when brighter' behaviour strongly supports this hypothesis. Although the global relationship between Γ and ξ in BHXRBs is well established by comparing measurements from single-epoch observations (e.g. Wu & Gu 2008; Younes et al. 2011), the correlation of Γ with ξ on short time-scales (within an observation, i.e. down to minutes or even seconds) is less well determined. However, Axelsson et al. (2008) showed for the BHXRB Cyg X-1 that the hardness–flux anticorrelation, seen in variations within an observation in brighter 'hard' states, becomes a positive correlation in the faintest 'hard' states. This change in behaviour is consistent with a positive Γ–ξ correlation at higher ξ changing to an anticorrelation at lower ξ, i.e. the variations within an observation follow the same trends as the global Γ–ξ relationship.

Theoretically, a considerable progress has been accomplished in this field with a better understanding of the complexity of the BHXRBs' 'hard state' as well as LLAGN (for a review see Narayan 2005). A currently proposed model involves an accretion disc plus a hot accretion flow model, the ADAF model, to explain the spectral dependence on the accretion rate for BHXRBs, from quiescence up to the 'soft state'. For intermediate accretion rates, as the accretion rate increases the Compton parameter in the hot accretion flow increases as well, producing a Comptonization X-ray spectrum with a 'harder' power-law slope. This regime is identified with the 'hard state', at mass accretion rates of 1–8 per cent of the Eddington rate, since the accretion process there is inefficient corresponding to lower fractions of $L_{\rm Edd}$, consistent with our observations of NGC 7213. As the accretion rate increases further, the model predicts a different behaviour in which increasing luminosity corresponds to 'softer' X-ray power-law slopes. This regime is identified with the 'soft state' and this is what is normally observed in higher luminosity AGN.

Finally, another interesting feature of the source's SED is the fact that its X-ray emission above 20 keV is quite high, and implies a high-energy cut-off larger than 350 keV (Lobban et al. 2010). NGC 7213 shows some weak evidence of a radio jet structure at 8.4 GHz (Blank, Harnett & Jones 2005). If such a structure is indeed there and it is aligned towards the observer's direction it could produce relativistically amplified radio emission through synchrotron radiation, and enhanced X-ray emission through inverse Compton radiation of either the synchrotron photons and/or optical photons from the starburst environment of the host galaxy. This possibility could explain the fact that the radio emission of the source lies between that of radio-loud and radio-quiet AGN, similar to blazars. At the same time, the existence of a jet could also account for the 'harder when brighter' behaviour of NGC 7213, something which is commonly observed in blazars (e.g. Krawczynski et al. 2004; Gliozzi et al. 2006; Zhang et al. 2006) and can be explained in the framework of the synchrotron self-Compton models. A jet model has also been proposed to explain the spectral evolution of the BHXRB XTE J1550−564 as it moves from the fading state towards the X-ray 'hard state' (Russell et al. 2010).

Therefore, a jet pointing towards us, contributing significantly to the radio and X-ray emission of the source, cannot be ruled out and, in fact, for the case of ADAF models, it can be created through the Blandford–Znajek mechanism (Armitage & Natarajan 1999). In the 'hard state' of BHXRBs, the kinetic luminosity in the jet is believed to equal the radiation luminosity (Fender, Gallo & Russell 2010). For the case of NGC 7213, assuming the existence of a jet, the previously derived accretion rate may therefore be lower by a factor of 2, still remaining well below the typical transition between the 'hard' and the 'soft' states in BHXRBs. In the future, models combining a jet component with a geometrically thin disc and ADAF (Yuan, Cui & Narayan 2005) need to be tested for the case of NGC 7213.

ACKNOWLEDGMENTS

DE and IMM acknowledge the Science and Technology Facilities Council (STFC) for support under grant ST/G003084/1. IEP acknowledges support by the EU FP7-REGPOT 206469 grant. PA acknowledges support from Fondecyt grant number 11100449. This research has made use of NASA's Astrophysics Data System Bibliographic Services. Finally, we are grateful to the anonymous referee for the useful comments and suggestions that helped improve the quality of the manuscript.

REFERENCES

Armitage P. J., Natarajan P., 1999, ApJ, 523, L7
Arnaud K. A., 1996, in Jacoby G. H., Barnes J., eds, ASP Conf. Ser. Vol. 101, Astronomical Data Analysis Software and Systems V. Astron. Soc. Pac., San Francisco, p. 17
Asmus D., Gandhi P., Smette A., Hönig S. F., Duschl W. J., 2011, A&A, 536, A36
Axelsson M., Hjalmarsdotter L., Borgonovo L., Larsson S., 2008, A&A, 490, 253
Bell M. E. et al., 2011, MNRAS, 411, 402
Belloni T., Homan J., Casella P., van der Klis M., Nespoli E., Lewin W. H. G., Miller J. M., Méndez M., 2005, A&A, 440, 207
Bevington P. R., Robinson D. K., 1992, Data Reduction and Error Analysis for the Physical Sciences, 2nd edn. McGraw-Hill, New York

Bianchi S., La Franca F., Matt G., Guainazzi M., Jimenez Bailón E., Longinotti A. L., Nicastro F., Pentericci L., 2008, MNRAS, 389, L52
Bird A. J. et al., 2010, ApJS, 186, 1
Blackburn J. K., 1995, in Shaw R. A., Payne H. E., Hayes J. J. E., eds, ASP Conf. Ser. Vol. 77, Astronomical Data Analysis Software and Systems IV. Astron. Soc. Pac., San Francisco, p. 367
Blank D. L., Harnett J. I., Jones P. A., 2005, MNRAS, 356, 734
Constantin A., Green P., Aldcroft T., Kim D.-W., Haggard D., Barkhouse W., Anderson S. F., 2009, ApJ, 705, 1336
Cusumano G. et al., 2010, A&A, 524, A64
Elvis M. et al., 1994, ApJS, 95, 1
Eracleous M., Hwang J. A., Flohic H. M. L. G., 2010, ApJS, 187, 135
Esin A. A., McClintock J. E., Narayan R., 1997, ApJ, 489, 865
Fender R. P., Gallo E., Russell D., 2010, MNRAS, 406, 1425
Filippenko A. V., Halpern J. P., 1984, ApJ, 285, 458
Gliozzi M., Sambruna R. M., Jung I., Krawczynski H., Horan D., Tavecchio F., 2006, ApJ, 646, 61
Gu M., Cao X., 2009, MNRAS, 399, 349
Heil L. M., Vaughan S., Uttley P., 2012, MNRAS, 422, 2620
Hönig S. F., Kishimoto M., Gandhi P., Smette A., Asmus D., Duschl W., Polletta M., Weigelt G., 2010, A&A, 515, A23
Isobe T., Feigelson E. D., Akritas M. G., Babu G. J., 1990, ApJ, 364, 104
Jahoda K., Swank J. H., Giles A. B., Stark M. J., Strohmayer T., Zhang W., Morgan E. H., 1996, in Siegmund O. H., Gummin M. A., eds, Proc. SPIE Vol. 2808, EUV, X-Ray, and Gamma-Ray Instrumentation for Astronomy VII. SPIE, Bellingham, p. 59
Kalberla P. M. W., Burton W. B., Hartmann D., Arnal E. M., Bajaja E., Morras R., Pöppel W. G. L., 2005, A&A, 440, 775
Körding E., Falcke H., Corbel S., 2006, A&A, 456, 439
Krawczynski H. et al., 2004, ApJ, 601, 151
Lamer G., McHardy I. M., Uttley P., Jahoda K., 2003, MNRAS, 338, 323
Lobban A. P., Reeves J. N., Porquet D., Braito V., Markowitz A., Miller L., Turner T. J., 2010, MNRAS, 408, 551
Maccarone T. J., 2003, A&A, 409, 697
McHardy I. M., Papadakis I. E., Uttley P., 1999, Nuclear Phys. B, 69, 509
Merloni A., Heinz S., di Matteo T., 2003, MNRAS, 345, 1057
Narayan R., 2005, Ap&SS, 300, 177
Narayan R., Yi I., 1994, ApJ, 428, L13
Nenkova M., Sirocky M. M., Nikutta R., Ivezić Ž., Elitzur M., 2008, ApJ, 685, 160
Peng C. Y., Ho L. C., Impey C. D., Rix H.-W., 2010, AJ, 139, 2097
Phillips M. M., 1979, ApJ, 227, L121
Press W. H., Teukolsky S. A., Vetterling W. T., Flannery B. P., 1992, Numerical Recipes in fortran: The Art of Scientific Computing, 2nd edn. Cambridge Univ. Press, Cambridge
Roy A. L., Norris R. P., 1997, MNRAS, 289, 824
Russell D. M., Maitra D., Dunn R. J. H., Markoff S., 2010, MNRAS, 405, 1759
Sault R. J., Teuben P. J., Wright M. C. H., 1995, in Shaw R. A., Payne H. E., Hayes J. J. E., eds, ASP Conf. Ser. Vol. 77, Astronomical Data Analysis Software and Systems IV. Astron. Soc. Pac., San Francisco, p. 433
Shao J., Tu D., 1995, The Jackknife and Bootstrap, 1st edn. Springer Series in Statistics. Springer, Berlin
Shemmer O., Brandt W. N., Netzer H., Maiolino R., Kaspi S., 2006, ApJ, 646, L29
Shields J. C., 1992, ApJ, 399, L27
Sobolewska M. A., Papadakis I. E., 2009, MNRAS, 399, 1597
Sobolewska M. A., Papadakis I. E., Done C., Malzac J., 2011, MNRAS, 417, 280
Starling R. L. C., Page M. J., Branduardi-Raymont G., Breeveld A. A., Soria R., Wu K., 2005, MNRAS, 356, 727
Tody D., 1993, in Hanisch R. J., Brissenden R. J. V., Barnes J., eds, ASP Conf. Ser. Vol. 52, Astronomical Data Analysis Software and Systems II. Astron. Soc. Pac., San Francisco, p. 173
Tully R. B., 1988, Nearby Galaxies Catalog. Cambridge Univ. Press, Cambridge, p. 221
Vaughan S., Edelson R., 2001, ApJ, 548, 694
Woo J., Urry C. M., 2002, ApJ, 579, 530
Wu Q., Gu M., 2008, ApJ, 682, 212
Wu C.-C., Boggess A., Gull T. R., 1983, ApJ, 266, 28
Younes G., Porquet D., Sabra B., Reeves J. N., 2011, A&A, 530, A149
Yuan F., Cui W., Narayan R., 2005, ApJ, 620, 905
Zhang Y. H., Treves A., Maraschi L., Bai J. M., Liu F. K., 2006, ApJ, 637, 699

This paper has been typeset from a TEX/LATEX file prepared by the author.